

# **Design of a WGM Ring Resonator Assisted Cancer Cell Detection System**

**Submitted By-**

**Bayzid**

**Student ID: 191116**

**Submitted To-**

Department of Electrical and Electronic Engineering  
in partial fulfillment of the requirements for the degree of Bachelor of Science in  
Electrical and Electronic Engineering.

**Supervised by-**

**Md. Rabiul Islam**

**Lecturer**

Department of Electrical and Electronic Engineering



**Jashore University of Science and Technology (JUST)**  
**Jashore-7408, Bangladesh**

**26 February 2025**

## DECLARATION

This is to certify that the thesis work entitled " **Design of a WGM Ring Resonator Assisted Cancer Cell Detection System** " has been carried out by **Bayzid** under the supervision of **Md. Rabiul Islam** in the Department of Electrical and Electronic Engineering, Jashore University of Science and Technology (JUST), Jashore, Bangladesh. The above thesis work or any part of this work has not been submitted anywhere for the award of any degree. The above declarations are true. Understanding these, this work has been submitted for the evaluation of an undergraduate thesis.

Signature of Supervisor  
Date:...../...../.....

Signature of Student  
Date:...../...../.....

## ACKNOWLEDGMENTS

First of all, I thank almighty Allah for keeping me physically and mentally fit during my thesis work. I would like to express my sincere gratitude to my Honourable supervisor **Md. Rabiul Islam**, Lecturer, Department of Electrical and Electronic Engineering, Jashore University of Science and Technology (JUST) for his continuous support, patience, motivation, enthusiasm and immense knowledge. His timely advice, meticulous security and scientific approach have helped me to a very great extent to accomplish this task. Then I would like to extend my gratitude to all other teachers, at Jashore University of Science and Technology (JUST) for their fruitful opinions and suggestions from time to time and their teaching and helping hand during the period of academic classes.

My heartiest thanks go to my family member **Md. Jahirul Islam**, Professor, Department of Electrical and Electronic Engineering, Khulna University of Engineering & Technology (KUET) for his continuous support, motivation, enthusiasm, immense knowledge and scientific approach have been invaluable in enabling me to successfully complete this task.

Finally, I would like to express thanks again for all of them mentioned above because I truly could not have done my work without them.

## ABSTRACT

Early detection of cancer is a vital role of patients to enhance the survival rates and furthermore to improve the treatment outcomes. Cancer in human life profoundly impacts not only human health but also mental, emotional, and social life. The traditional diagnosis methods like chemical analysis and surgical biopsies are expensive, and time-intensive. Moreover, it causes physical discomfort and psychological distress for patients. To overcome these challenges, the whispering gallery mode (WGM) ring resonator is a more efficient and cost-effective biosensor device. Biosensors based on optical phenomena including absorption, scattering, reflectance, and transmittance emerged as highly promising technologies. The WGM ring resonator is a non-invasive, rapid, and reliable alternative to conventional diagnosis methods. The proposed WGM Ring Resonator has the potential to exhibit high sensitivity for detecting different cancer cells such as blood, skin, cervical, adrenal gland and breast. It detects by analyzing the variation of refractive index according to the plasma in affected cells. The designed biosensor device significantly enhances its performance by comprising ring waveguides coupled with two straight waveguides. The Sensitivity (S) and Quality factor (Q) can be improved by increasing the light-analyte interaction length into the two straight waveguides.

In this work, a highly optimized Whispering Gallery Mode (WGM) Ring Resonator (RR) is a specially designed target particle(plasma) acceptor layer deposited on the inner surface of the straight waveguide. In a straight waveguide, the resonant light interacts with target plasma molecules, resulting in a change in the resonating mode of effective Refractive Index (RI). This innovative approach is set to effectively detect and quantify the presence of cancer in affected cells. The proposed WGM ring resonator is numerically analyzed using the finite element method encapsulated in COMSOL Multiphysics to identify the resonator's spectral response. However, it measures the resonance wavelength according to the change in refractive index (RI). The optical and structural parameters of the proposed ring resonator-based biosensor are comprehensively studied and optimized to enhance its effectiveness in detecting cancer cells. A detailed analysis demonstrates that a ring resonator with a simplified structural architecture and optimized parameters will significantly increase sensitivity in the detection of cancer cells.

The optimized Ring Resonator-based Biosensor shows a high sensitivity(s) of 400 nm/RIU with a quality factor (Q) of 47.2 for skin cancer cells (Basal) according to the change in RI from (1.36 to 1.38). The simulation and analysis demonstrate the high sensitivity(S) of cervical cancer cells (Hela) is found at 1571nm/RIU and the Quality factor(Q) is 31.5 with RI changes from (1.368 to 1.392). For the Blood cancer cells (Jurkat) shows the sensitivity(S) of 500 nm/RIU and the quality factor(Q) 45 according to the change in RI from (1.376 to 1.390). Again, the biosensor for Adrenal Gland cancer cells (PC-12) detection shows excellent sensitivity(S) is 1175nm/RIU and Quality factor(Q) is 33 with variations of RI (1.381 to 1.395). Finally, the proposed biosensor displays high sensitivity(S) 500nm/RIU and the Quality factor(Q) 42 according to the change in RI (1.385 to 1.399) for Breast cancer cells (MDA-MB-232) detection.

This study showed that the proposed biosensor achieved higher sensitivity than other Silicon Photonics Ring Resonators, Nanocavity-Coupled Photonic Crystal Waveguide, and multi-core whispering gallery mode bio-sensors.

**Keywords: WGM, Ring Resonator, Photonics, Cancer cell, Sensitivity, Quality Factor.**

# TABLE OF CONTENTS

Title Page	i
Declaration	ii
Acknowledgments	iii
Abstract	iv
Tables of contents	vi
List of Tables	viii
List of Figures	ix
List of Abbreviations & Symbols	xi
Dedicated	xii
<b>CHAPTER 1      Introduction</b>	<b>1</b>
1.1 Introduction	1
1.2 Background of the WGM Resonator	1
1.3 Review of Literature	2
1.4 Motivation	3
1.5 The Objectives and Aims of Research	4
<b>CHAPTER 2      Whispering Gallery Mode Resonators Biosensor</b>	<b>5</b>
2.1 Introduction	5
2.2 Biosensor	5
2.2.1 Optical Biosensor	6
2.2.2 Electrical Biosensors	8
2.3 Benefits and Drawbacks of WGM Ring Resonator	9
2.4 Applications of WGM Resonators	10
<b>CHAPTER 3      Optical Ring Resonator Design And Modeling</b>	<b>11</b>
3.1 WGM Ring Resonator-Based Biosensor To Detect Cancer Cells	11
3.1.1 Optical Ring Resonator	11
3.1.2 Geometry and Numerical Design for Waveguide	12
<b>CHAPTER 4      Ring Resonator Design Procedure</b>	<b>16</b>
4.1 System Parameter Selection of WGM Ring Resonator	16
4.2 Geometry and Parameter Selection	20

<b>CHAPTER 5</b>	<b>Numerical Results and Discussion</b>	23
	5.1 Biosensor-based WGM Ring Resonator for Cancer Cell Detection	23
	5.1.1 Sensitivity of designed Biosensor for detection of Blood cancer cells	24
	5.1.2 Sensitivity of designed Biosensor for detection of Skin cancer cells	26
	5.1.3 Sensitivity of designed Biosensor for detection of Cervical cancer cells	28
	5.1.4 Sensitivity of designed Biosensor for detection of Adrenal Gland cancer cells	30
	5.1.5 Sensitivity of designed Biosensor for detection of Breast cancer cells	32
	5.2 Comparison Between WGM Ring Resonator, Silicon Photonics Ring Resonator, And Nanocavity-Coupled Photonic Crystal Waveguide, and multi-core whispering gallery mode bio-sensor.	34
	5.3 Discussion	37
<b>CHAPTER 6</b>	<b>Conclusion and Future Work</b>	38
	6.1 Conclusion	38
	6.2 Future Work	38
<b>References</b>		39
	<b>Appendix A</b>	42

## LIST OF TABLES

<b>TableNo.</b>	<b>Description</b>	<b>Page</b>
4.1	Parameter optimized for core diameter Selection	16
4.2	Parameter optimized for cladding Thickness Selection	17
4.3	Parameter optimized for Radius of Curvature Selection	18
4.4	Parameter optimized for Separation Between Waveguide Selection	18
4.5	Final Parameter optimized for Waveguide design In COMSOL Multiphysics.	19
4.6	Basic Parameter of the proposed Ring Resonator.	20
4.7	Parameter of the proposed Ring Resonator (Blood Cancer Cell)	21
4.8	Parameter of the proposed Ring Resonator (Skin Cancer Cell)	21
4.9	Parameter of the proposed Ring Resonator (Cervical Cancer Cell)	21
4.10	Parameter of the proposed Ring Resonator (Adrenal Gland Cancer Cell)	22
4.11	Parameter of the proposed Ring Resonator (Breast Cancer Cell)	22
5.2.1	Sensitivity and Quality Factor of the Designed WGM Ring Resonator for Detecting Different Cancer Cells.	34
5.2.2	Sensitivity and Quality Factor of the Designed Silicon Photonics Ring Resonator for Detecting Different Cancer Cells	35
5.2.3	Sensitivity and Quality Factor of the Designed Nanocavity-Coupled Photonic Crystal Waveguide for Detecting Different Cancer Cells.	35
5.2.4	Sensitivity and Quality Factor of the Designed multi-core whispering gallery mode bio-sensor for Detecting Different Cancer Cells.	36



## LIST OF FIGURES

<b>Figure No</b>	<b>Description</b>	<b>Page</b>
1.1	(a) St. Paul's Cathedral View in London. (b) The Sketch of Whispering Gallery.	2
1.2	The Sound strength path in a circular whispering gallery.	2
2.1	Schematic representation of biosensor design and transducing mechanism.	6
3.1	Schematic design of the Ring Resonator-based Biosensor.	12
3.2	The proposed WGM Ring Resonator System	13
3.3	Cross-section of the proposed WGM ring resonator according to parameter selection.	14
3.4	The Mesh Schematic representation used in the COMSOL Multiphysics simulations.	15
5.1	The electric field distribution in the WGM Ring Resonator.	23
5.2	Transmittance characteristics of the proposed sensor, adding bioparticles the refractive index changes from 1.376 to 1.390.	25
5.3	Shift in resonance wavelength due to shift in RI.	25
5.4	Change in amplitude of the transmittance curve due to change in RI.	26
5.5	Transmittance characteristics of the proposed sensor, adding bioparticles the refractive index changes from (1.36 to 1.38).	27
5.6	Shift in resonance wavelength due to shift in RI.	27
5.7	Change in amplitude of the transmittance curve due to change in RI.	28
5.8	Transmittance characteristics of the proposed sensor, adding bioparticles the refractive index changes from (1.368 to 1.392).	29
5.9	Shift in resonance wavelength due to shift in RI.	29
5.10	Change in amplitude of the transmittance curve due to change in RI.	30

5.11	Transmittance characteristics of the proposed sensor, adding bioparticles the refractive index changes from (1.381 to 1.395).	31
5.12	Shift in resonance wavelength due to shift in RI.	31
5.13	Change in amplitude of the transmittance curve due to change in RI.	32
5.14	Transmittance characteristics of the proposed sensor, adding bioparticles the refractive index changes from (1.385 to 1.399).	32
5.15	Shift in resonance wavelength due to shift in RI.	33
5.16	Change in amplitude of the transmittance curve due to change in RI.	33

## List of Abbreviations & Symbols

B.W.	3dB bandwidth of the spectral response
FEM	Finite Element Method
FRET	Forester resonance energy Transfer
FTIR	Fourier transform infrared spectroscopy
LOD	limit of detection
Q-factor	Quality Factor
RI	Refractive Index
RR	Ring Resonator
S	Sensitivity
SARS-CoV-2	Corona Virus-2
SPR	Surface Plasmon Resonator
TIR	Total internal reflection
UV-vis	Ultraviolet-visible spectroscopy
WGM	Whispering Gallery Mode
$L_{eff}$	Effective interaction length in $\mu m$
$\lambda_{res}$	resonance wavelength

## **DEDICATED**

This thesis work is wholeheartedly dedicated to my beloved parents and family members, who have been my source of inspiration. To my siblings, relatives, mentors, friends and classmates who shared their words of advice and encouragement to finish this study.

And lastly, I also dedicated this work to the almighty Allah, thank you for the guidance, strength, power of the mind, protection and skills and for giving us a healthy life. All of these, I offer to you.

# **CHAPTER I**

## **Introduction**

### **1.1 Introduction**

Whispering gallery mode (WGM) is one kind of wave that can travel around a concave surface. It occurs when waves such as electromagnetic, acoustic, or optical can propagate along the concave surface due to total internal reflection (TIR). The TIR occurs when the resonator exhibits higher optical density (e.g. higher RI) compared to the surrounding medium. TIR occurs when the incident angle of light rays relative to the surface is equal to the critical angle. When light approaches an angle near  $90^\circ$  it remains in close proximity to the surface. This close proximity allows the light to effectively interfere with itself. After completing a round trip within the dielectric medium, the constructive interference leads to the formation of resonances. The total internal reflection in WGM resonators is highly effective in minimizing energy loss. While some losses may occur when guided waves are in close proximity to the surface, potentially causing diffusion. The primary sources of these losses are intrinsic material absorption and surface roughness. Despite these factors, the loss coefficients of nonlinear material (e.g. silicon dioxide) are impressively low.

A significant advantage of WGM resonators is their capability to attain extremely high Sensitivity(S) and high Quality factor(Q). The Sensitivity(S) refers to the ability of the resonator to detect small variations of Refractive index(RI). The Q factor is inversely proportional to the total loss in the system. As the losses decrease, the resonator efficiency increases. These Characteristics improve their performance and potential applications in various fields. However, in this chapter, we discuss about background of the WGM Resonator, review of literature, motivation, and the objectives and aims of research.

### **1.2 Background of the WGM Resonator**

Lord Rayleigh formally used the term WGM in architectural structures found below the St.Paul Cathedral dome in 19<sup>th</sup> century. It was identified that a whisper sound coming from one end of the dome could still be heard clearly at the other end, a considerable distance from the source (see Fig1.1). Rayleigh discovered that sound wave also travels along the dome concave surface [1]. The dome's concave surface prevents to expand as fast as the beam cross section while propagating its free space. On the other hand, the beam cross-section increases, resulting in a proportional decrease in radiation intensity relative to the square of the distance from the source [1].

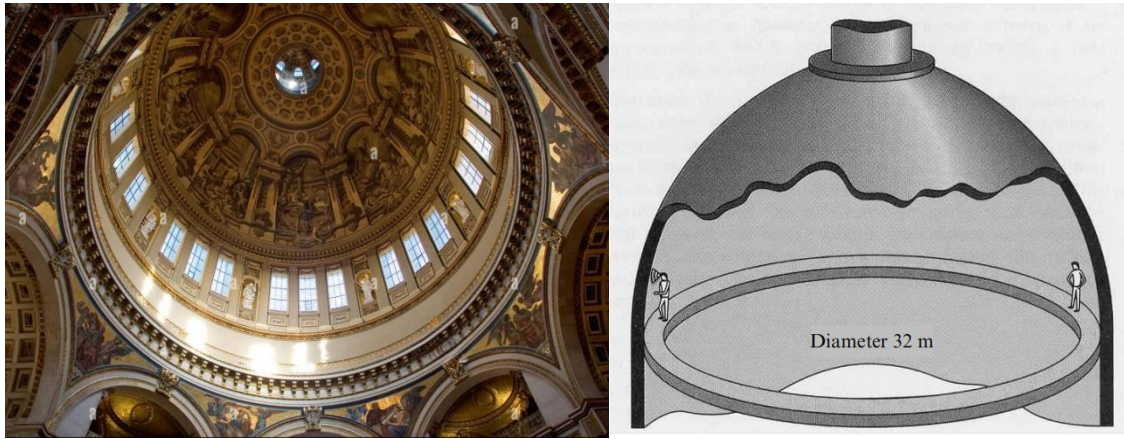


Fig. 1.1 (a) St. Paul's Cathedral View in London [2].(b) The Sketch of Whispering Gallery [1]. In the whispering gallery, the radiation propagates within a narrow layer that closely adheres to the wall surface (see Fig 1.2). Within this layer, the sound intensity decreases directly proportional to the distance [1].

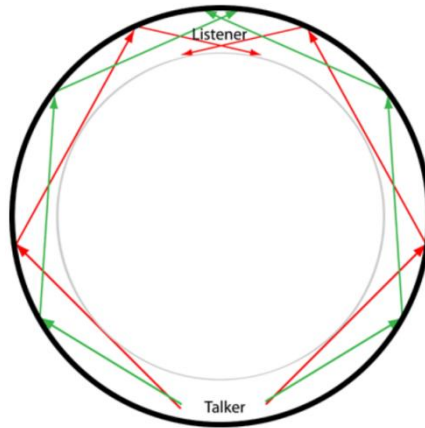


Fig. 1.2 The Sound strength path in a circular whispering gallery.

Early in the 20<sup>th</sup> century, it was evident that electromagnetic waves could exist within a dielectric sphere. Which exhibits a spatial structure that closely resembles with whispering gallery acoustic waves. However, the extensive research began on this phenomenon in the 1990s, resulting in successive implementations of whispering gallery modes in the fields of optics [1].

### 1.3 Review of Literature

The Thesis work is demonstrating substantial progress in the field of Biosensor Technologies. Biosensor devices offer label-free profiling of pharmacological properties used in drug discovery, diagnostics, and life sciences [3]. A range of sensing designs including mechanical, electrical, magnet, thermometric, and optical has been incorporated into the biosensor [4]. Biosensors provide early diagnosis and infection surveillance by detecting coronavirus 2 (SARS-CoV-2) focusing on viral antigens [5]. The Detection efficiency is improved by

developments in nanotechnology, microfluidics, and biosensor-based optical, mechanical, electro-chemical and nano-biosensors [5]. Polymeric Whispering gallery micro-lasers are highly effective laser biosensors that provide high accuracy in the detection of proteins. In both air and solution, these free-space photonic micro-sensors require no waveguides and function [6]. The Ring resonator sensors have significant applications in environmental monitoring, food safety, pharmaceuticals, and healthcare sectors. These sensors highly offer rapid and responsive analytical tools inspired by extensive research in this area [7],[8]. High Q optical sensors including micro-cavities and photonic crystals significantly improve molecular sensing capabilities [8]. Micro Ring Resonators are widely used for detecting biological equivalents [8],[9], Such as Thrombin detection [10],[11], Vascular endothelial growth factor detection [11], and Biochemical compounds [10]. In addition, notable applications include chemical sensing [10], detection of blood proteins, optical filtering, routing, delay lines [11], corrosion detection [12], and toxic sensing [13]. Optical ring resonators, basically in all pass and add-drop configurations are utilized for detecting of bioparticles like DNA and proteins. Which can effort to ensure food safety [14].

The biosensor-based WGM Ring resonator is used for the detection of hemoglobin (HB) in Blood samples. This one straight waveguide coupled with ring waveguide biosensor devices achieves high-quality factor and sensitivity [15]. The analysis of fiber ring transmission characteristics measuring intensity transmission and phase shift. Which demonstrates a tunable true time delay element from such a resonator [16]. A hybrid D-type photonic crystal fiber sensor composed of gold, graphene, and Ti3C2Tx-MXene. This sensor effectively utilizes surface plasmon resonance to achieve high sensitivity and cost-effective detection of cancer cells [17]. A silicon photonics ring resonator-based biosensor exhibits high sensitivity and selectivity for detecting different cancer cells, such as leukemia, cervical cancer, and breast cancer [31]. A bio-sensing platform based on a nanocavity-coupled photonic Crystal waveguide (PCW) is proposed for diseased cell detection using a label-free waveguide [33].

#### 1.4 Motivation

- Analyzing the literature review we find some limitations or research gaps which are comparatively low sensitivity and accuracy.
- Refractive index (RI) measurement techniques such as fluorescence measurement, and refract meter have many drawbacks including fabrication complexity, bulky size, and costly component requirements.
- Optical fiber sensors are immune to electromagnetic interference, high sensitivity, and tiny in size, with fiber grating sensors widely used for measuring strain, temperature, pressure, gas or liquid flow, PH, and even plant and human beings [18].
- WGM Ring Resonator represents advanced technological solutions with Compact design and High sensitivity.
- In this Research, we aim to design and analyze a WGM Ring Resonator coupled with two straight waveguides on both sides of the ring waveguide for high sensitivity(S) and Quality factor(Q).

## 1.5 The Objectives and Aims of Research

The main objective of this thesis is to enhance and effectively address the fundamental aspects related to the development of novel sensors and tunable devices based on WGM Ring Resonators. By focusing on these elements, the research aims to improve these systems close to the practical applications. In addition, this initiative aims to highly sensitive ring resonator devices for sensing applications through optical Whispering Gallery Modes.

The specific objectives of this research are as follows:

- ❖ To design highly sensitive optical WGM ring resonator devices to enhance sensing applications.
- ❖ Achieving high Sensitivity(S) and good Quality factor(Q) to evaluate and optimize the design parameters.
- ❖ Analyzed the effective refractive index(RI) and transmission characteristics of the proposed Ring Resonator using COMSOL Multiphysics.
- ❖ The proposed simulation-based sensor is used to detect cancer cells using plasma samples.
- ❖ Compare the results obtained from two straight waveguides coupled with a ring and the single straight waveguide coupled with a ring.
- ❖ Compare the achieved results with other Silicon Photonics Ring Resonators, Nanocavity-Coupled Photonic Crystal waveguides, and multi-core whispering gallery mode biosensors.



## CHAPTER 2

# Whispering Gallery Mode Resonators Biosensor

### 2.1 Introduction

This section, provides a brief overview of key theoretical concepts related to resonators, with a special focus on Whispering gallery mode (WGM) Resonators in the linear regime. WGM resonators are optical and electromagnetic devices that confine and circulate light or sound through total internal reflection (TIR). First, we outline the resonance conditions and spectral response of traveling wave resonators, which helps to represent some important parameters (i.e. sensitivity(s), quality factor(Q)). Next, we look at the specific case of the WGM dielectric resonators analyzing their model structure in terms of dispersion and field distribution. Field distribution information allows for the clarification of the techniques that couple external electromagnetic waves to the WGM resonator from outside. Whispering gallery modes or waves inside a resonator (a cavity) refer to specific resonance modes with smooth and curved boundaries. These modes are applied in various wave types such as electromagnetic and sound waves. When waves (i.e. light, sound) enter the cavity, they undergo continuous total internal reflection (TIR) along the curved surface according to the resonance condition. After completing a full round trip within the resonator, the waves return to their original position with the same phase and thereby interact with each other constructively and formation of waves standing. These resonances significantly influence the geometry of the resonator cavity. The size, shape, and material properties of the resonator determine the specific resonance frequencies and the efficiency of wave confinement. One of the key advantages of WGM resonators is their label-free sensing capability, where small changes in the surrounding environment can shift resonance conditions. This makes them ideal for detecting biological molecules, temperature variations, and chemical substances. Additionally, they are widely used in applications such as laser stabilization, nonlinear optics, and frequency comb generation to showcase their versatility. As a result, precise control over resonator design is essential for detecting and optimizing performance in applications such as optical communication, sensing, and quantum technologies. WGM resonators offer high sensitivity, compact size, and strong light confinement, making them valuable for a variety of scientific and technological applications.

### 2.2 Biosensor

The founding father of the biosensor is Leland C. Clark. Jr, Biochemist of the United States 1956 [19]. His innovative creation known as the Clark oxygen electrodes was designed to measure the concentration of oxygen within biological systems. This biosensor consisted of an electrochemical cell that utilized an oxygen-permeable membrane. Which facilitates the

diffusion of oxygen to be reduced at a platinum cathode. The resulting electrical current is directly proportional to the oxygen concentration which provides accurate measurement. Biosensors are analytical devices that mixture of elements for biological detection with a sensor system and transducer [20]. As compared to the available diagnostic systems, biosensors offer improved sensitivity and selectivity to make them highly effective in various applications.

Biosensors play an important role in monitoring biological emissions within the agriculture and food sectors. These advanced tools help to detect harmful pathogens, toxics, and contaminants present in soil, water, and crops. By enabling early detection of diseases in plants and animals to improve food safety and improving agricultural yield. Similarly, Biosensors are used to monitor food quality, detect spoilage, and ensure adherence to safety regulations.

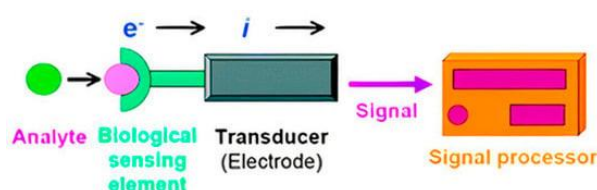


Fig 2.1. Schematic representation of biosensor design and transducing mechanism [21].

Biosensors can be categorized according to the mechanism by which the unit converts the adsorption of substances into detectable signals. According to this classification, four primary types of biosensors exist such as optical, electrical, mechanical, and magnetic. The sensing technologies can be classified into two distinct types to enhance the interaction with the detector. Firstly, the analyte or target species is to be labeled with a specific chemical group or entity. Secondly, The direct detection facilitates of an unlabeled analyte through its interaction with the sensor. In some sensing methodologies, detection limits may be inadequate without the application of signal amplification. However, most of the literature on biosensors focuses on 'label-free' sensing technologies.

The necessity for specification in detection often complicates chemical labeling difficult, costly, and sometimes impractical, especially when analyzing complex biological samples such as blood, and plasma. The potential for unintended interactions can result in inaccurate outcomes. As a response to these challenges, label-free biosensing has gained a more efficient and reliable approach for detecting biomolecular interactions. However, label-free biosensors offer significant advantages in research and diagnostic applications.

### 2.2.1 Optical Biosensors

Optical biosensors detect changes in light signals caused by the light-analyte interaction. It is detected by various methods like as the spectroscopy method, Fluorescence method, and Surface plasmon Resonance (SPR). The spectroscopic method called Fourier transform infrared (FTIR) spectroscopy and Ultraviolet-visible (UV-vis) spectroscopy distinguishes the

signal from the analyte. Fluorescent-based detection is the most popular method in analytical applications [22]. It occurs when a molecule absorbs a photon of light and then releases another photon at a lower energy level. This emitted light can be measured to identify and quantify with high sensitivity. Optical biosensors are valuable in various fields such as environmental monitoring, medical diagnosis, and food safety. Their ability to provide real-time, highly accurate detection makes their importance as essential tools in modern analytical applications. Molecules with electric structures that allow efficient excitation and emission of light within the visible to near-infrared spectrum are known as fluorophores. Certain species exhibit reduced fluorescence when exposed to a certain wavelength of light, thereby enhancing more suitable for the use of fluorophores in particular experimental conditions.

The application of optical elements to remove background and excitation radiation. Which enables the separation and collection of fluorescence signals using detectors (e.g. photocell, photoconductive avalanche, photodetector tunnel, or device coupled with charge). However, there are two primary limitations to fluorescence measurements using fluorescently labeled species. Firstly, adding the analyte to a fluorescent tag can influence the binding interactions during specific sensing events. which is especially significant for proteins whose configurations may be adversely disrupted by the presence of fluorophores. This is widely compared to smaller molecule analytes. Secondly, the reliability of quantitative fluorescence measurements may be unreliable and compromised at extreme analyte concentrations. At low concentrations scenarios, the signal to noise ratio (SNR) may be longer than the dominant factor in determining the limit of detection (LOD). Instead, light from sources unrelated to the fluorophores can contribute more to the signal than the analyte.

Therefore, at low levels of the signal-to-background ratio (SBR), not the SNR also affects the precision of the measurement. The distance between two freely moving objects at high concentrations in order for excited fluorophores to transfer their energy to a neighboring fluorophore. The fluorescently labeled analyte molecules can be quite small. Although this is frequently discussed in terms of an incoming photon exciting additional fluorophores, the energy transfer does not include radiation. This process refers to the conversion of Forester resonance energy (FRET) and can be used to record the similarities between two fluorophores. Higher concentrations also contribute to frequent mutual interactions between the solution biomolecules and aggregation in certain animals. The particles produced may diffuse adequate lighting to decrease the excitation of fluorophores present or the amount of fluorescence emitted that can reach the detector. However, for measurements of fluorescence at high concentrations, a roughly low signal may be measured. The sandwich assay commonly employs the fluorescence method used for biosensing. In this type of experiment, the sample solution is specifically bound to a substrate through a binding molecule that has the surface of a well or other cell that has been covalently immobilized. Otherwise, alternative fluorescence assays differ from conventional biochemical techniques such as Western blots or assays that were performed from Enzyme-linked immunosorbent assay (ELISA) to modern sensor methods such as TIRF [23].

The second category of optical biosensors uses changes in the light phase to report the presence of the analyte rather than amplitude variations (i.e. absorption). A significant advantage of switching frequency-based optical biosensors is that they do not require labeling to identify resonance, making them simpler and more efficient. While spectroscopic techniques rely on weak interactions between light and the analyte (or label) unless a selected wavelength is to report transformation phase-based detection that requires a comparison of refractive index changes. However, for transformation detection, this approach enhances sensitivity without needing specific wavelengths. In comparison, by using one effective method interferometry calculating phase shifts is measured to improve accuracy and reduce noise. This strategy is exemplified by Backscatter Interferometry [22], which allows for precise detection of molecular interactions. In some cases, the detector can show a harmonic function over time, with its frequency which can be connected to the path length difference. These phase-based optical biosensors offer high sensitivity, label-free detection, and reduced background noise, making them valuable for real-time monitoring in medical diagnostics, biochemical research, and environmental analysis.

### **2.2.2 Electrical Biosensors**

Biosensors that detect changes in a system's electrical properties due to proximity or analyte interactions have become common and appreciate the advantages of using raw electrical signals [22]. These raw electrical can be directly processed such as current or impedance [22]. The field effect transistor (FET) based biosensors are the most promising due to their high sensitivity and real-time detection capabilities. FETs are instruments, that are embedded in semiconductor materials, control the source, and drain are considered the current between two electrical edges. The current flowing between these two terminals is influenced by an applied electric field, which serves as the gate. In biosensing applications, charged biomolecules immobilized on the sensor's semiconductor surface generate this electric field, that functions as the gate and becomes different from the density of the charge carrier inside the carrier. The resultant drain current can be easily measured, which makes FET biosensors highly effective for detecting molecular interactions.

However, conventional FET biosensors have a limitation in that their limit of detection (LOD) is typically greater than 1 nanometer. This is because the electric field from the bound species only penetrates inside the conduction channel to a small depth. To overcome this challenge, the use of nano-scale artifacts for bridging the source, and drain such as carbon nanotubes [24] and lithographically defined nanowires [25]. These nanostructures offer an improved surface area-to-volume ratio, causing the electric field to interact with a larger portion of the conduction channel. As a result, these nanoscale FET biosensors can achieve significantly lower LOD, to enable single virus particles to be detected [26]. Another key advantage of nanowire FET biosensors is their compatibility with low-cost microfabrication techniques commonly used in the semiconductor industry. They are label-free devices meaning that they do not require chemical tagging of the target molecules to simplify the sensing process. Their small size

makes them ideal for integration into microfluidic systems where only small sample volumes (in the microliter range) are required for testing.

One of the primary challenges in nanowire Field-Effect Transistor (FET) biosensors is their reduced efficiency in the presence of salts. Most biomolecules typically require a buffered atmosphere to maintain their stability and function, meaning that pH-buffered salt solutions are also used to dissolve known analyte samples. For this reason, also biological fluids such as blood and serum naturally contain salts and buffering agents.

These salts create a screening effect, which diminishes the influence of the biomolecule's electrical field on the conductor charge carrier population [22]. As a result, the sensitivity of the biosensor is significantly reduced when used with biologically relevant fluids. This screening effect weakens the interaction between surface-bound biological macromolecules and the sensor limiting precise detection.

Another issue is that surface modifications of the nanowire which are often necessary for targeted sensing may enhance conductivity, depending on the electrical properties of the nanowire. Furthermore, any functionalization schemes may also permanently alter the nanowire's charge state which affects its fundamental electrical properties and overall sensor performance [10]. It remains challenging to find methods sufficient to overcome these limitations in the field of nanowire FET biosensors. Recently, clever techniques have been used to boost the applicability of these instruments [27].

### **2.3 Benefits and Drawbacks of WGM Ring Resonator**

The Whispering Gallery Mode (WGM) Ring Resonator-based biosensor offers several advantages in biomedical sensing, particularly for cancer detection. One of the most significant benefits is its high sensitivity, as it can detect minute changes in the refractive index (RI), enabling early-stage cancer detection with superior accuracy. Additionally, WGM-based sensors exhibit a high-quality factor (Q), leading to sharp and well-defined resonance peaks, which enhance measurement precision. Another advantage is the real-time and label-free detection capability. Unlike traditional methods that rely on chemical markers or fluorescent labels, WGM biosensors can directly detect biomolecular interactions, reducing sample preparation complexity and potential errors. Micron-sized monolithic transparent dielectric structures are optical whisper gallery mode (WGM) resonators in which closed light paths are assisted using absolute inner reflections from circular boundaries [28]. The possible resonance of light can be contained within a compact cavity that has low mode volumes and high-quality factors (Q) by utilizing optical technologies like photodiodes and optical fibers. A WGM sensor can be developed as a more affordable and flexible sensor [29].

Furthermore, WGM ring resonators are compact, lightweight, and integrable with lab-on-a-chip systems, making them suitable for point-of-care diagnostics. Their non-invasive nature

minimizes patient discomfort, offering a promising alternative to biopsies and chemical analysis. Despite their advantages, WGM ring resonators also have limitations. One major challenge is their high susceptibility to environmental fluctuations, such as temperature variations and mechanical vibrations, which can cause resonance shifts and impact measurement accuracy. To address this, sophisticated stabilization mechanisms or reference sensors may be required, increasing system complexity.

The WGM sensor is temperature sensitive so a temperature controller is needed for field work [30]. Fabrication challenges remain significant, as achieving high precision in the resonator's geometry is critical to maintaining desired Q factors. Even minor imperfections can lead to scattering losses, thereby degrading performance. Another drawback is the fabrication complexity and cost. Achieving precise micro/nanostructure fabrication with low surface roughness is critical for optimal performance, but this requires advanced manufacturing techniques, increasing production expenses. Moreover, coupling light efficiently into and out of these resonators can be technically demanding and may introduce additional losses or alignment complexities. The sensitivity to surface conditions, while beneficial for sensing, may also render the device vulnerable to contamination and aging, necessitating stringent environmental control and maintenance. Additionally, WGM biosensors are highly sensitive to non-specific binding, which may lead to false-positive or false-negative results, necessitating improved surface functionalization strategies. The sensitivity to surface conditions, while beneficial for sensing, may also render the device vulnerable to contamination and aging, necessitating stringent environmental control and maintenance.

In conclusion, while WGM ring resonators offer remarkable sensitivity and real-time detection capabilities, challenges related to environmental stability, fabrication costs, and specificity must be addressed to fully realize their potential in clinical diagnostics.

## **2.4 Applications of WGM Resonators**

Due to their characteristics and potential as novel sensors, optical resonators have gained a great deal of interest over the past few years. Intensive study in this area is motivated by enormous applications in diverse fields of resonator sensors. Several applications of WGM resonators in different fields are enlisted below in details.

## CHAPTER 3

### Optical Ring Resonator Design And Modeling

#### 3.1 WGM Ring Resonator-Based Biosensor to Detect Cancer Cells

Biochemistry and genetics need rapid development to expand the use of different medical instruments and apparatus for preventing, detecting, and sensing diseases. Early cancer detection and diagnosis depend on improving treatment outcomes and patient survival. However, conventional cancer diagnosis techniques like chemical analysis and surgery are not only costly and time-consuming but may also traumatize patients. A key priority in modern medical research is developing a highly sensitive, affordable, and user-friendly cancer detection device. The WGM ring resonator system shines brightly as an innovative solution, utilizing light that travels around a concave surface. This technology promises to enhance early cancer detection capabilities significantly.

In this section, we describe the configuration of WGM ring resonators to identify cancer cells using cell plasma. Numerical studies are performed routinely to define the spectral response of the resonator and then calculate the shift of the resonance wavelength consequent upon changing the plasma samples' RI. The structural and optical parameters of the proposed biosensor based on a ring resonator are closely studied and similarly optimized for making the biosensor ideal for the successful detection of cancer cells using cell plasma samples. The ring resonator would achieve greater sensitivity with optimized design parameters and simple structural architecture. The designed optimized biosensor-based ring resonators display a very high sensitivity(S) and good quality factor (Q).

##### 3.1.1 Optical Ring Resonator

Ring resonators are typically designed and fabricated in two distinct models. The first model involves an optical fiber configuration, where a ring resonator is achieved by connecting the ends of an optical fiber. An additional optical fiber is then employed to efficiently couple light into the ring [31]. The second model features integrated optical structures, developed through advanced integrated optics technology. Resonators developed using this method demonstrate not only remarkable reliability but also outstanding repeatability [14].

On the other hand, a ring resonator is a set of waveguides that must have one ring waveguide coupled with one or more straight waveguides (see figure 3.1). The optical ring resonator analyzes variations in light behavior resulting from the interaction of electromagnetic waves with biological molecules such as proteins, bacteria, cells, or DNA samples to identify the

target molecules [14]. The change in the light's behavior is directly caused by the interaction between the evanescent field of the resonating light inside the resonator and the ambient bioparticles [14].

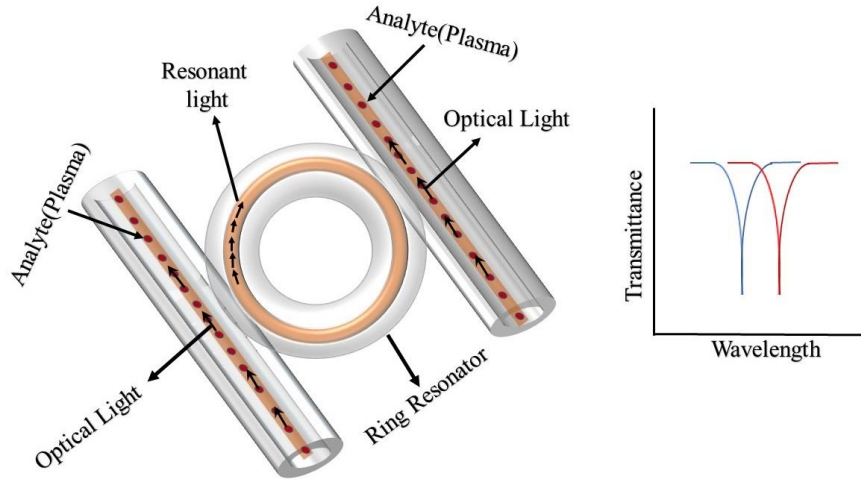


Fig 3.1: Schematic design of the Ring Resonator-based Biosensor.

It is noted that the plasmapheresis process, followed by the centrifuge, is used to extract plasma from blood cells [15].

Cancer is a complex disease defined by the abnormal and uncontrolled increases of cells and the spread of these cells to various tissues and organs within the body. Cancer in human life profoundly impacts human health, mental, emotional, and social life which requires easy and early detection for proper treatment and lifesaving issues. The ring resonator's performance for detecting Blood, Cervical, Adrenal gland, Skin, and Breast cancer cells can be evaluated by examining its sensitivity and quality factor, particularly focusing on the RI of optical light.

### 3.1.2 Geometry and Numerical Design for Waveguide

In this analysis, the Finite element method is used in which the 2D geometry of the WGM ring resonator is built in COMSOL Multiphysics. The schematic of the ring resonator is shown in Figure 3.2.



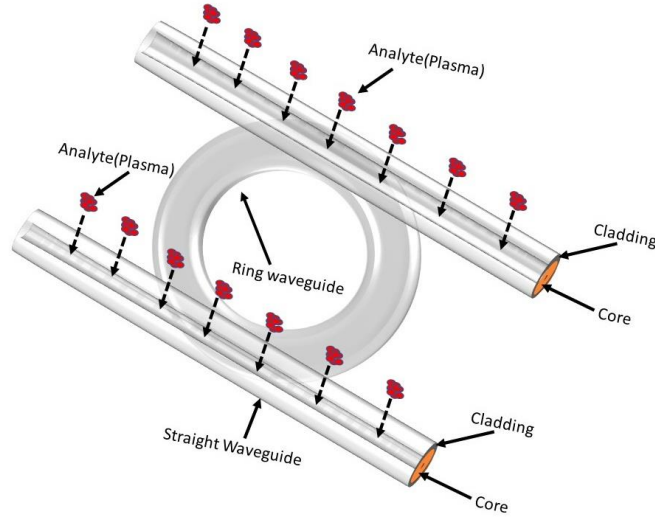


Fig 3.2: The proposed WGM Ring Resonator System.

The optical ring resonator sensor effectively harnesses the interaction between light and analyte in the two straight waveguides that are coupled to the ring. The light that passes through the two straight waveguides couples to the ring and resonance occurs. Which must meet the following conditions [10],[32],[15],

$$m\lambda_{res} = 2\pi R\eta_{eff} \quad (3.1)$$

Where,  $m$ =integer number,  $\lambda_{res}$  = resonance wavelength in  $\mu m$ ,  $R$  = the ring radius in  $\mu m$  and  $\eta_{eff}$  =effective refractive index. The optical path length of the ring resonator is aligned with an integer multiple of the resonance wavelength ( $\lambda_{res}$ ) for resonance to be established, as outlined in Equation (3.1). This condition is essential for achieving constructive interference of light waves circulating within the ring, which ultimately leads to an amplification of the signal strength. The resonant light confidently circulates along the ring resonator, exhibiting a strong evanescent field that ensures the light-analyte interaction length is effectively equal to the physical length of the sensor.

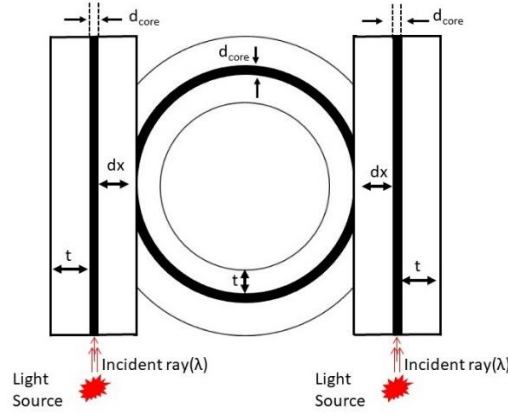


Fig 3.3. Cross-section of the proposed WGM ring resonator according to parameter selection.

This unique circulating nature of the resonant mode results in an exceptionally long effective interaction length, determined by [15],[33],

$$L_{eff} = \frac{Q\lambda_{res}}{2\pi\eta_{eff}} \quad (3.2)$$

Here,  $Q$  = quality factor,  $L_{eff}$  = *effective interaction length in  $\mu m$* . The quality factor of the resonator is a critical parameter that measures the efficiency of the light circulating within the ring resonator. A higher  $Q$  factor suggests that the light can complete a greater number of circulations, thereby enhancing the interaction with the analyte through an extended effective interaction [31].

The quality factor defined by

$$Q = \frac{\lambda_{res}}{B.W.} \quad (3.3)$$

Where  $\lambda_{res}$  = resonance wavelength and B.W. = 3dB bandwidth of the spectral response respectively [14].

It is important to recognize that the value of effective interaction length ( $L_{eff}$ ) typically increases as the Quality factor( $Q$ ) rises. The  $Q$  factor is a key measure of the system's performance, with higher values indicating improved resonance. Therefore, the 'goodness' of the system can be measured using the  $Q$  factor of the ring resonator system. A higher  $Q$  factor results in a narrower bandwidth for this quality estimation, which is highly advantageous for

many applications requiring signal filtering and minimal energy loss. The Mesh Schematic Representation in COMSOL Multiphysics (see Figure 3.4) refers to the structured discretization of a computational domain used for the finite element method. This representation ensures numerical analysis in solving simulated geometry. The mesh consists of elements such as tetrahedral, hexahedral, prismatic, or triangular connected through nodes that define the computational framework. A mesh in COMSOL is characterized by its element type, size, and refinement strategy. Element quality is determined by parameters like skewness, aspect ratio, and growth rate, ensuring convergence and stability. The adaptive meshing feature refines elements based on error estimation, optimizing computational efficiency.

To investigate the result in COMSOL Multiphysics need to select an appropriate mesh. The smaller mesh sizes generally improve performance but at the cost of longer computation times and higher memory usage. we employed a free triangular mesh for our simulations shown schematic view in Figure (3.4).

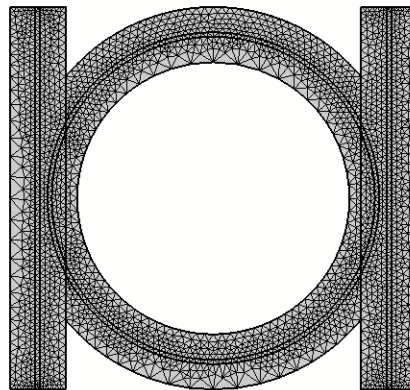


Fig.3.4: The Mesh Schematic representation used in the COMSOL Multiphysics simulations.

The appropriate boundary conditions are one of the significant prerequisites for obtaining accurate results in the finite element method. Properly simplifying the defined boundary conditions not only streamlines the simulation process but also significantly enhances its performance.

## CHAPTER 4

### Ring Resonator Design Procedure

#### 4.1 System Parameter Selection of WGM Ring Resonator

We employ COMSOL Multiphysics to effectively build the 2D ring resonator model. Which uses the finite element method to enhance our analytical capabilities and improve the design process. The initial geometrical parameters of the system that are selected based on the Q-factor are shown in the table (4.1 to 4.5). For each parameter, various datasets were analyzed and the optimal combination was chosen to achieve the quality factor and high sensitivity ensuring enhanced system performance.

Table 4.1: Parameter optimized for core diameter Selection.

Core diameter ( $\mu\text{m}$ )	Cladding thickness ( $\mu\text{m}$ )	Radius of the curvature ( $\mu\text{m}$ )	Separation between waveguide ( $\mu\text{m}$ )	Quality Factor(Q)
0.17	2.100	6.200	0.450	42
0.18	2.100	6.200	0.450	43
0.19	2.100	6.200	0.450	43
0.20	2.100	6.200	0.450	45
0.21	2.100	6.200	0.450	38
0.22	2.100	6.200	0.450	45
0.23	2.100	6.200	0.450	33

In this examination, we have systematically investigated the Q factor for 8 different core diameters shown in Table 4.1. The numerical simulations were conducted using COMSOL Multiphysics where the maximum Q factor is 45 was achieved with a core diameter of 0.2  $\mu\text{m}$ . However, the simulations were performed under specific design parameters such as a cladding

thickness of 2.100  $\mu\text{m}$ , a radius of curvature of 6.200  $\mu\text{m}$ , and a waveguide separation of 0.450  $\mu\text{m}$ . These parameters were carefully chosen to ensure high sensitivity and high performance in the numerically designed structure for cancer cell detection. The high-quality factor(Q) enhanced optical confinement and reduced propagation losses. which are critical for precise and reliable biosensing applications.

Table 4.2: Parameter optimized for cladding Thickness Selection.

<b>Core diameter (<math>\mu\text{m}</math>)</b>	<b>Cladding thickness (<math>\mu\text{m}</math>)</b>	<b>Radius of curvature (<math>\mu\text{m}</math>)</b>	<b>Separation between waveguide (<math>\mu\text{m}</math>)</b>	<b>Quality Factor(Q)</b>
0.20	2.020	6.200	0.450	38
0.20	2.050	6.200	0.450	43
0.20	2.070	6.200	0.450	40
0.20	2.100	6.200	0.450	45
0.20	2.200	6.200	0.450	40
0.20	2.220	6.200	0.450	37

In this study, we examined distinct Quality factors across seven different cladding thicknesses shown in detail in Table 4.2. The results demonstrate that we achieved a maximum Quality factor of 45 with a cladding thickness of 2.100  $\mu\text{m}$  with a core diameter of 0.20  $\mu\text{m}$ , a radius of curvature of 6.200  $\mu\text{m}$ , and a separation of 0.450  $\mu\text{m}$  between the waveguides for the numerically designed Cancer cell detection devices. However, the maximum Quality Factor is the same as Table 4.1 in core and the clad parameters value is also the same.

Table 4.3: Parameter optimized for Radius of Curvature Selection.

<b>Core diameter (<math>\mu\text{m}</math>)</b>	<b>Cladding thickness (<math>\mu\text{m}</math>)</b>	<b>Radius of curvature (<math>\mu\text{m}</math>)</b>	<b>Separation between waveguide (<math>\mu\text{m}</math>)</b>	<b>Quality Factor(Q)</b>
0.20	2.100	6.190	0.450	31
0.20	2.100	6.200	0.450	42
0.20	2.100	6.220	0.450	40
0.20	2.100	6.230	0.450	45
0.20	2.100	6.240	0.450	39
0.20	2.100	6.250	0.450	37

In Table 4.3, we have checked the quality factor(Q) for the selection of radius of curvature. The numerical simulations were conducted using COMSOL Multiphysics where the maximum Q factor is 45 was achieved. However, the simulations were performed under specific design parameters such as a core diameter of 0.20  $\mu\text{m}$ , a cladding thickness of 2.100  $\mu\text{m}$ , and a waveguide separation of 0.450  $\mu\text{m}$ . These parameters are selected to maximize sensitivity and performance in the numerically designed structure for cancer cell detection. The quality factor (Q) significantly improves optical confinement and minimizes propagation losses, ensuring precise and reliable output.

Table 4.4: Parameter optimized for Separation Between Waveguide Selection.

<b>Core diameter (<math>\mu\text{m}</math>)</b>	<b>Cladding thickness (<math>\mu\text{m}</math>)</b>	<b>Radius of curvature (<math>\mu\text{m}</math>)</b>	<b>Separation between waveguide (<math>\mu\text{m}</math>)</b>	<b>Quality Factor(Q)</b>
0.20	2.100	6.200	0.430	31
0.20	2.100	6.200	0.433	37

0.20	2.100	6.200	0.445	40
0.20	2.100	6.200	0.450	45
0.20	2.100	6.200	0.475	39
0.20	2.100	6.200	0.490	32

Table 4.4 shows the maximum quality factor for various changes in separation between waveguide selections. We also investigate the Quality factor for 6 different values. Then we get the maximum quality factor is 45 for the value of two waveguide separations is 0.450  $\mu\text{m}$ . However, the simulations were performed under these design parameters including a core diameter of 0.20  $\mu\text{m}$ , a cladding thickness of 2.100  $\mu\text{m}$ , and a radius of curvature of 6.200  $\mu\text{m}$ . The parameters have been selected to optimize sensitivity and performance in the numerically designed structure. The enhancement of the quality factor (Q) has significantly improved optical confinement while minimizing propagation losses.

Table 4.5: Final Parameter optimized for Waveguide design In COMSOL Multiphysics.

<b>Core diameter (<math>\mu\text{m}</math>)</b>	<b>Cladding thickness (<math>\mu\text{m}</math>)</b>	<b>Radius of curvature (<math>\mu\text{m}</math>)</b>	<b>Separation between waveguide (<math>\mu\text{m}</math>)</b>	<b>Quality Factor(Q)</b>
0.17	2.020	6.190	0.430	33
0.18	2.050	6.200	0.433	45
0.19	2.070	6.220	0.445	40
0.20	2.100	6.230	0.450	45
0.21	2.200	6.240	0.475	38
0.22	2.220	6.250	0.490	43

In this investigation, we analyze several Q for a suitable combination of core diameter, clad thickness, Radius of curvature, and separation between Waveguide shown in detail in Table 4.5. The numerical simulations were conducted using COMSOL Multiphysics where the maximum Q factor is 45 was achieved by designing cancer cell detection devices. However, the simulations were performed under specific design parameters such as a core diameter of 0.20  $\mu\text{m}$ , a cladding thickness of 2.100  $\mu\text{m}$ , and a waveguide separation of 0.450  $\mu\text{m}$ . The parameters have been selected to optimize sensitivity and performance in the numerically designed structure. The enhancement of the Q has significantly improved optical confinement while minimizing propagation losses and enhancing reliability.

#### 4.2 Geometry and Parameter Selection

We use COMSOL Multiphysics to design the 3D geometry of the WGM Ring Resonator by Finite element Method. The diagram of the Ring Resonator is shown in Fig 3.3 and Table 4.6 provides the final selected geometrical parameters of the devices for (blood, skin, cervical, adrenal gland, and breast) cancer cell detection.

Table 4.6: Basic Parameter of the proposed Ring Resonator.

Parameter	Value
Wavelength( $\lambda$ )	1550nm
Core diameter( $d_{\text{core}}$ )	200nm
Cladding width( $t$ )	2100nm
The radius of the Curvature( $r$ )	6200nm
Separation between Core( $dx$ )	450nm
Operating frequency ( $f$ )	$1.9341 \times 10^{14}$ Hz

The proposed ring resonator has been specifically designed to enhance the detection of blood cancer cells by effectively responding to variations in the refractive index ranging from 1.376 to 1.390(see Table 4.7). This precise range is suitable as it correlates to the optical properties of blood cancer cells and allows for improved sensitivity and accuracy in identifying these cells



amidst healthy tissue. The sensor's ability to operate within this refractive index range positions it as a significant tool in early diagnosis and monitoring of blood cancer and leads to better patient outcomes.

Table 4.7: Parameter of the proposed Ring Resonator (Blood Cancer Cell)

Parameter	Value
RI range of straight waveguide core (ncore_st)	1.376-1.390
Core RI (n_core)	1.39007
Cladding RI (n_clad)	1.256

This study is carefully designed to significantly enhance the detection of Skin cancer cells. It achieves this by effectively responding to variations in the refractive index, specifically within the range of 1.36 to 1.38(see Table 4.8). This precise refractive index range is particularly relevant, as it aligns closely with the optical characteristics of skin cancer cells, allowing for a substantial increase in both sensitivity and accuracy.

The proposed sensor enables it to operate optimally within this targeted refractive index range from 1.368 to 1.392(see Table 4.9) positioning it as an essential instrument for the early diagnosis and ongoing monitoring of skin cancer. By facilitating the detection of cancerous cells at an earlier stage, this technology has the potential to lead to improved patient outcomes, making it a crucial advancement in medical diagnostics.

Table 4.8: Parameter of the proposed Ring Resonator (Skin Cancer Cell)

Parameter	Value
RI range of straight waveguide core (ncore_st)	1.36-1.38
Core RI (n_core)	1.38007
Cladding RI (n_clad)	1.24

Table 4.9: Parameter of the proposed Ring Resonator (Cervical Cancer Cell)

Parameter	Value
RI range of straight waveguide core (ncore_st)	1.368-1.392
Core RI (n_core)	1.39207
Cladding RI (n_clad)	1.248

In Table 4.10 and Table 4.11, The proposed ring resonator based on a biosensor has been intricately designed to significantly enhance the detection of Adrenal gland cancer cells and breast cancer cells. It achieves a remarkable responsiveness to variations in the refractive index, which is an essential range of 1.381 to 1.395, and 1.385 to 1.399. This particular range aligns with the unique optical properties of blood cancer cells, allowing for higher sensitivity and precision in distinguishing these malignant cells from surrounding healthy tissue.

Table 4.10: Parameter of the proposed Ring Resonator (Adrenal Gland Cancer Cell)

Parameter	Value
RI range of straight waveguide core (ncore_st)	1.381-1.395
Core RI (n_core)	1.39507
Cladding RI (n_clad)	1.261

Table 4.11: Parameter of the proposed Ring Resonator (Breast Cancer Cell)

Parameter	Value
RI range of straight waveguide core (ncore_st)	1.385-1.399
Core RI (n_core)	1.39907
Cladding RI (n_clad)	1.265

The sensor's extraordinary ability to operate within this refractive index range establishes it as an invaluable asset in the early diagnosis and continuous monitoring of blood cancer, thereby the way for improved patient outcomes and potentially transformative advances in clinical care.

## CHAPTER 5

### Numerical Results and Discussion

#### 5.1 Biosensor-based WGM Ring Resonator for Cancer Cell Detection

This research discusses the development and application of biosensors based on whispering gallery mode (WGM) ring resonators specifically designed for the sensitive detection of cancer cells. The innovative design of these biosensors leverages the unique optical properties of WGM resonators enhancing detection capabilities and presenting significant potential for advancements in medical diagnostics and monitoring. The spectral response of the designed optical ring resonator for cancer cells was numerically analyzed using COMSOL Multiphysics. The design of the proposed sensor (Figure 5.5) was created using COMSOL Multiphysics. The study investigates the resonator's spectral behavior and sensitivity within an all-pass configuration. The proposed ring resonator is constructed with silicon dioxide. This configuration is to be chosen to optimize the resonator's performance in detecting Cancer cells in the human body. The numerical simulations focus on the resonator's wavelength shifts and produce high sensitivity to variations in the refractive index of the surrounding medium. The spectral response is essential for understanding the ring resonator's ability to detect even small changes in the refractive index. Here, We describe the coupling of light into and out of the resonator in terms of a generalized beam splitter.

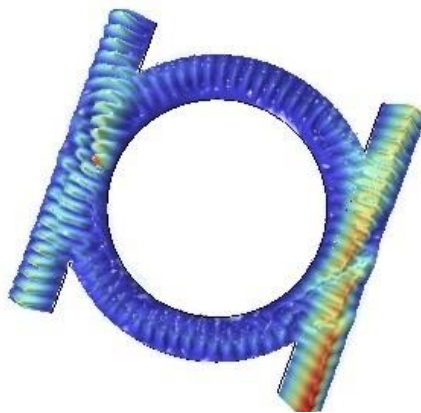


Fig. 5.1: The electric field distribution in the WGM Ring Resonator.

In the WGM, the intensity transmission factor is used to determine the transmission characteristics which is given by

$$T = \left[ \frac{E_2}{E_1} \right]^2 = \frac{\tau^2 - 2r\tau \cos\varphi + r^2}{1 - 2r\tau \cos\varphi + r^2\tau^2} \quad (5.1)$$

Here,  $E_1$  and  $E_2$  are the input and output electric fields. The script ( $\varphi$ ) represents the round trip phase while a  $\tau$  denotes the reflectance and transmittance components that require  $r^2 + \tau^2 = 1$  [16].

The proposed WGM ring resonator was numerically analyzed using the finite element method using COMSOL Multiphysics. The change in refractive index (RI) indicates the interaction of light with the target plasma molecules, which is crucial for detecting blood cancer cells effectively. The slight variations in RI can significantly impact the resonating modes within the ring resonator, allowing for precise identification and analysis of cancerous cells. When the plasma is injected into the active layer of the straight waveguide of the ring resonator, the resonant light interacts with target plasma molecules, resulting in a change in the resonating mode of effective RI. The sensitivity of the proposed sensor was evaluated using the following relationship [34],[15],

$$S = \frac{\Delta\lambda_{res}}{\Delta RI} \quad (5.2)$$

Where,  $\Delta\lambda_{res}$ =change in resonance wavelength and  $\Delta RI$  =change in refractive index.

Extensive investigations show that due to the interaction between the plasma and the evanescent fields resonance conditions may occur. An example of such electric field distribution is shown in Fig.5.1.

### 5.1.1 Sensitivity of designed Biosensor for detection of Blood cancer cells

In this study, Fig.5.2. illustrates the significant change in resonance frequency corresponding to the maximum range of refractive index change (1.376 to 1.390) observed in the proposed ring resonator. Further investigations show that the resonance wavelength shifts when the RI changes [see Fig. 5.3]. From the analysis, the maximum wavelength sensitivity of the blood cancer cells (Jurkat) shows 500 nm/RIU. This indicates that two straight waveguide systems

show better sensitivity compared to a single straight waveguide coupled with a ring waveguide achieving a sensitivity of 361 nm/RIU [15].

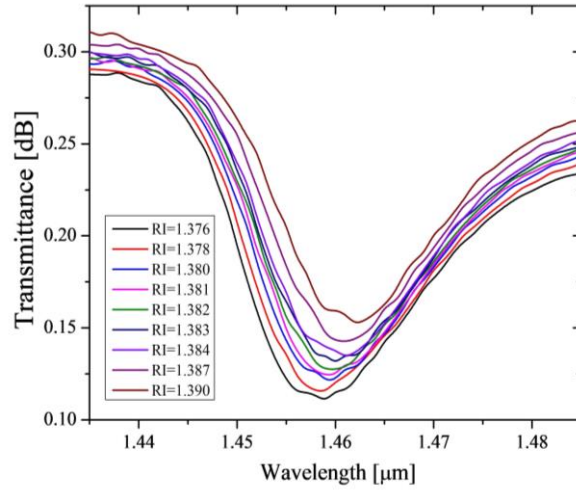


Fig.5.2: Transmittance characteristics of the proposed sensor, adding bioparticles the refractive index changes from 1.376 to 1.390.

However, by implementing two straight waveguides on either side of the ring waveguide, we significantly improve the sensitivity of the system. This configuration allows for greater interaction between the light and the surrounding medium, resulting in improved detection capabilities for variations in RI.

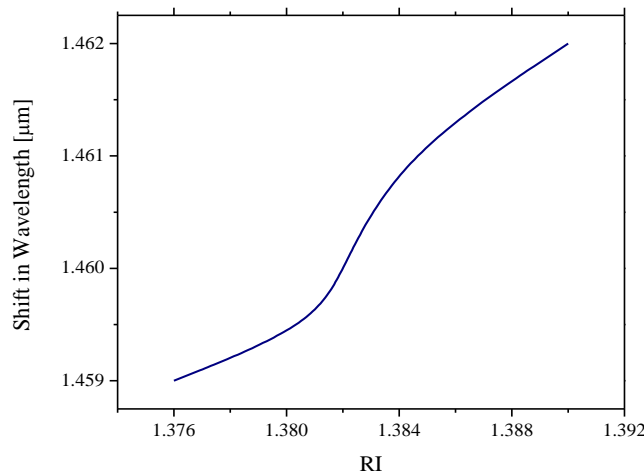


Fig.5.3: Shift in resonance wavelength due to shift in RI.

As the concentration of plasma increases in the two straight waveguides, it effectively alters the RI of the sample, leading to a corresponding change in the amplitude of the transmittance curve as is shown in Fig. 5.4. in the ring resonator.

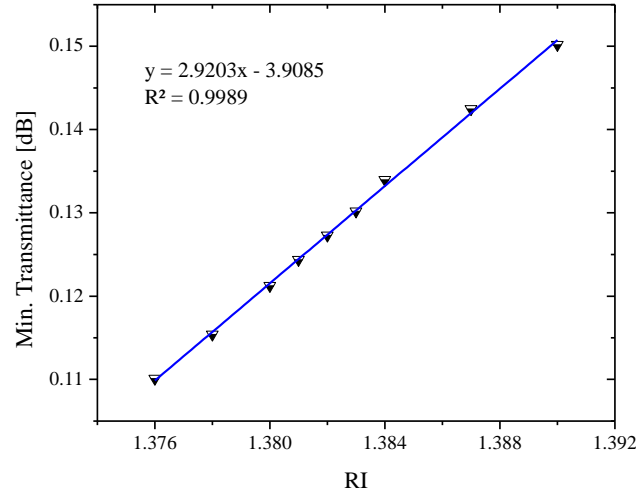


Fig.5.4: Change in amplitude of the transmittance curve due to change in RI.

As is shown in Fig. 5.4, the change is completely linear ( $R^2 = 0.9989$ ), which demonstrates the sensor's suitability for the detection process. Finally, the quality factor is also determined which was found 45 lower than 1143[15]. As a result, the proposed ring resonator has a low quality factor but it offers high sensitivity which significantly enhances the sensor's detection capability and stability.

### 5.1.2 Sensitivity of designed Biosensor for detection of Skin cancer cells

The significant change in resonance frequency corresponds to the maximum refractive index variation, ranging from 1.36 to 1.38, observed in the proposed ring resonator shown in Fig.5.5. This design optimizes high wavelength sensitivity for detecting Skin cancer cells (Normal, Basal) with a sensitivity of 400 nm/RIU. In comparison, the sensitivities previously reported for the Normal (healthy) and the Basal (cancerous) cells are 223.41nm/RIU [34], 650nm/RIU [35], and 388.8nm/RIU [36]. Further investigations show that the resonance wavelength shifts when the RI changes [see Fig. 5.6].

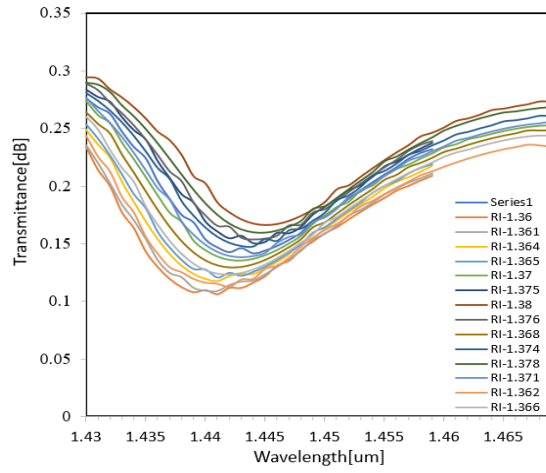


Fig.5.5: Transmittance characteristics of the proposed sensor, adding bioparticles the refractive index changes from (1.36 to 1.38).

From the analysis, the maximum wavelength sensitivity of the Skin cancer cells shows 400 nm/RIU.

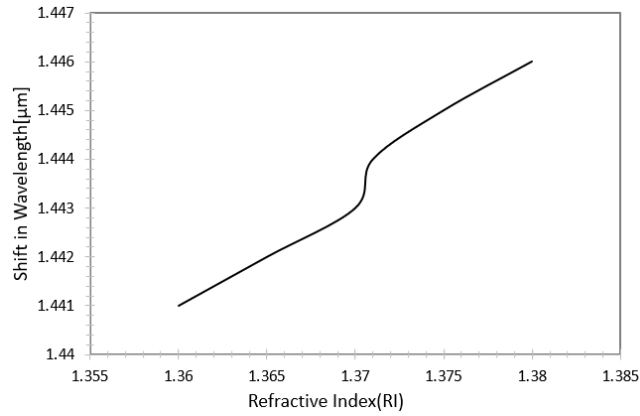


Fig.5.6: Shift in resonance wavelength due to shift in RI.

The increase of plasma concentration in the two straight waveguides leads to a significant change in the amplitude of the transmittance curve (see Figure 5.7), it effectively changes the RI of the sample. The change is near to linear which demonstrates the sensor's capability for the detection process.

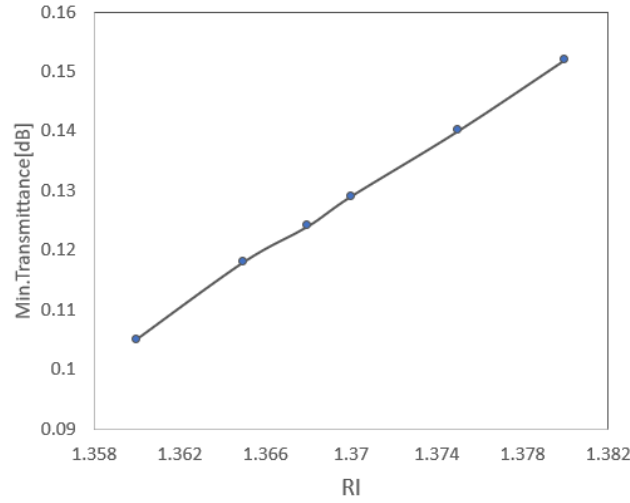


Fig.5.7: Change in amplitude of the transmittance curve due to change in RI.

The introduction of two straight waveguides coupled with the ring waveguide enhances the system's sensitivity significantly. This arrangement facilitates increased interaction between the light and analyte(plasma), which leads to improved detection capabilities for variations in refractive index (RI). Finally, the quality factor is 47.2 to be determined by investigating the value of core, clad, separation between the waveguide, and radius of the curvature parameters less than 59.97 [34]. As a result, the proposed ring resonator has a lower quality factor but it offers high sensitivity that can significantly increase the capability of the device.

### 5.1.3 Sensitivity of designed Biosensor for detection of Cervical cancer cells

The proposed ring resonator indicates a significant shift in resonance frequency corresponding to a refractive index change from 1.368 to 1.392 shown in Fig 5.8. This proposed design optimizes high wavelength sensitivity for detecting Cervical cancer cells (Normal, Hela) with a sensitivity of 1571 nm/RIU. Comparatively, the sensitivities previously reported for the Normal (healthy cell) and the Hela (cancerous cell) cells are 225.51nm/RIU [34], 666nm/RIU[35], and 390.75nm/RIU [36]. However, these results indicate that the proposed ring resonator design offers higher sensitivity for cancer cell detection.



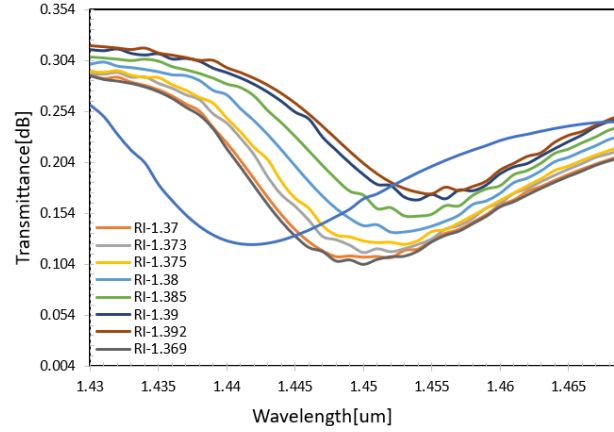


Fig.5.8: Transmittance characteristics of the proposed sensor, adding bioparticles the refractive index changes from (1.368 to 1.392).

Fig.5.9 shows a relation, in which the resonance wavelength shift takes the RI 1.368 as a base and adds concerning resonance wavelength changes due to RI change for 1.373, 1.375, 1.38, 1.385, 1.392. The RI has been taken in a range (1.368 to 1.392) due to cervical cancer cells(plasma) RI changes in this range.

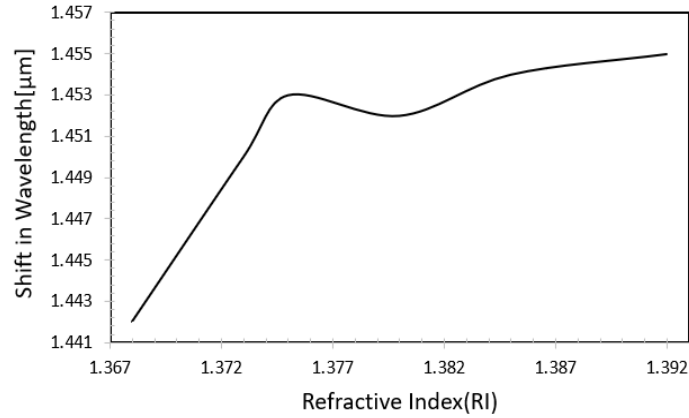


Fig.5.9: Shift in resonance wavelength due to shift in RI.

The concentration of plasma increases in the two straight waveguides, it effectively alters the RI of the sample. The ring resonator leads to a corresponding change in the amplitude of the transmittance curve as is shown in Fig. 5.10. As is shown in Fig. 5.10, the change is close to

linear which demonstrates the sensor's suitability for the detection process. By placing two straight waveguides on both sides of the ring waveguide, we significantly enhance the sensitivity of the devices. This configuration increases light-analyte interaction between the light and the plasma in the straight waveguide, enabling improved detection capabilities for variations in refractive index (RI).

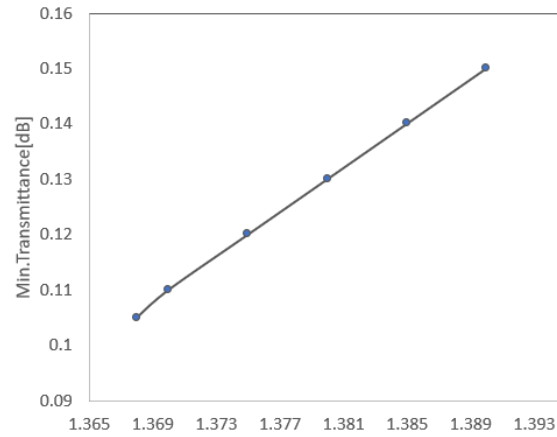


Fig.5.10: Change in amplitude of the transmittance curve due to change in RI.

Finally, the sensitivity was significantly high 1571nm/RIU, and the quality factor was also determined which was 31.5 less than 62.27 [34]. However, the proposed ring resonator has a lower quality factor but it offers high sensitivity which significantly enhances the sensor's detection capability and stability.

#### 5.1.4 Sensitivity of designed Biosensor for detection of Adrenal Gland cancer cells

The noticeable change in resonance frequency according to the significant change of refractive index (RI) in the proposed ring resonator, is depicted in Fig.5.11. This advanced biosensor device demonstrates remarkable sensitivity, achieving 1175nm/RIU when detecting Adrenal Gland Cancel Cells, including both normal(healthy) and PC-12(cancerous) cells. Previous research has reported varying sensitivities of 226.22nm/RIU [34], and 390.95nm/RIU [36] which is significantly less than these proposed biosensor devices.

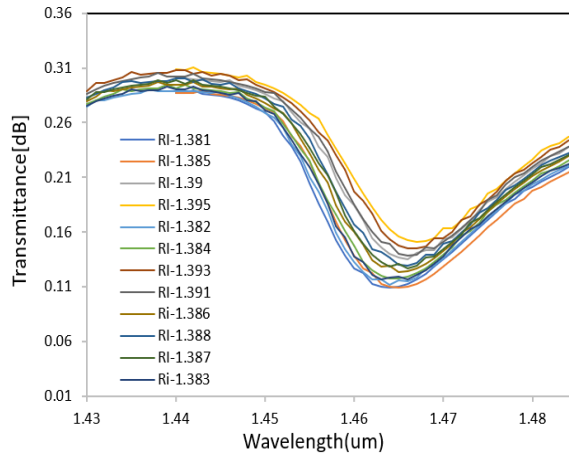


Fig.5.11: Transmittance characteristics of the proposed sensor, adding bioparticles the refractive index changes from (1.381 to 1.395).

The resonance wavelength shift takes the RI 1.381 as a base and adds concerning resonance wavelength changes due to RI change for 1.381, 1.382, 1.385, 1.387, and 1.393 shown in Fig.5.12. The RI has been taken in a range (1.381 to 1.393) due to adrenal cancer cells(plasma) RI changes in this range. The concentration of plasma increases in the two straight waveguides, it effectively alters the RI of the sample. The ring resonator leads to a corresponding change in the amplitude of the transmittance curve as is shown in Fig. 5.13.

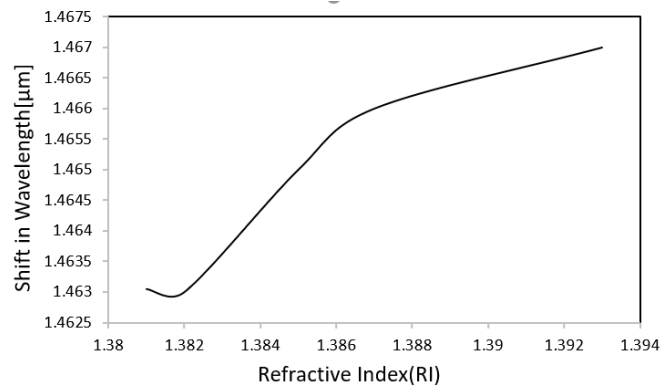


Fig.5.12: Shift in resonance wavelength due to shift in RI.

This arrangement also increased interaction between the light and analyte(plasma), which leads to improved detection capabilities for variations in refractive index (RI). However, the quality factor is obtained at 33 to be determined by investigating the value of core, clad, the

separation between the waveguide, and the radius of the curvature parameters which is less than 62.05 [34].

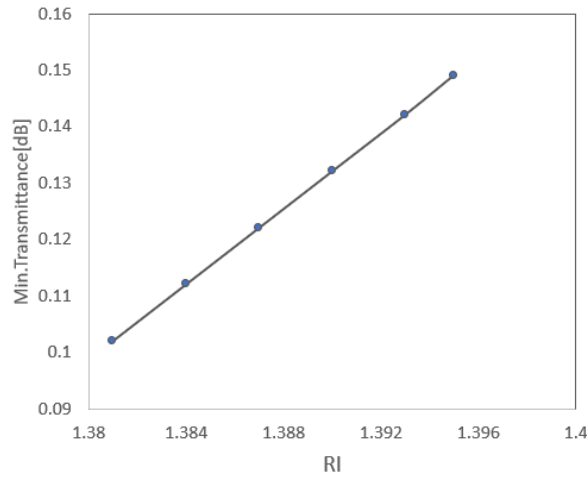


Fig.5.13: Change in amplitude of the transmittance curve due to change in RI.

As a result, the proposed ring resonator has a low quality factor but it offers high sensitivity which significantly enhances the sensor's detection capability and stability.

### 5.1.5 Sensitivity of designed Biosensor for detection of Breast cancer cells

The slight change is the refractive index (RI) which occurs with the significant change in resonance frequency shown in (figure 5.14) in the proposed ring resonator. The biosensor-based ring resonator devices optimize the wavelength sensitivity(S), reaching an impressive 500nm/RIU for detecting breast cancer cells (Normal, MDA-MB-231). Comparatively, the previous research has reported sensitivities for normal(healthy) and MDA-MB-231(cancerous)

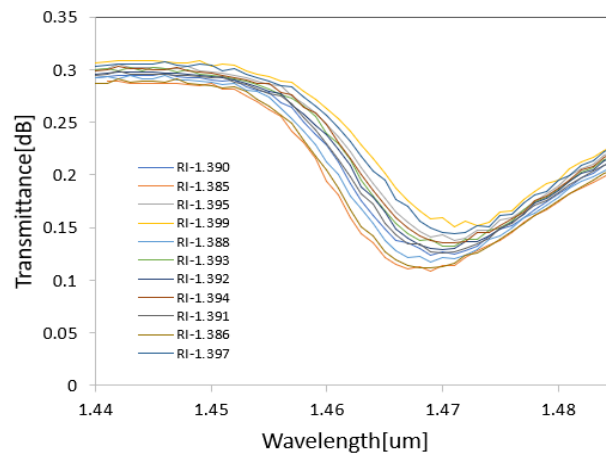


Fig.5.14: Transmittance characteristics of the proposed sensor, adding bioparticles the refractive index changes from (1.385 to 1.399).

cells, measured at 227.54nm/RIU [34], 642.857nm/RIU [35], and 391.45nm/RIU [36]. However, the proposed ring resonator wavelength sensitivity is comparatively better than that of other proposed designs.

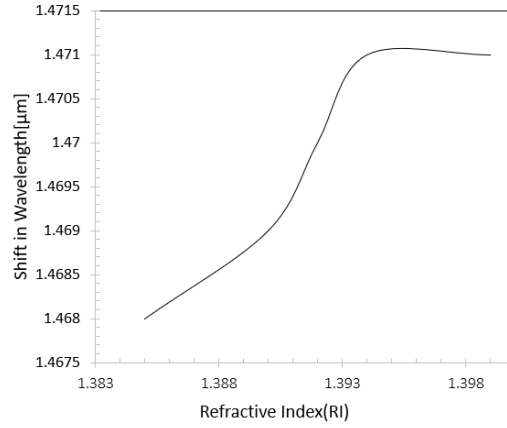


Fig.5.15: Shift in resonance wavelength due to shift in RI.

The resonance wavelength shifted according to RI change for 1.385, 1.390, 1.392, 1.394, and 1.399 shown in Fig.5.15. The RI has been taken in a range (1.385 to 1.399) due to adrenal cancer cells(plasma) RI changes in this range.

The plasma concentration is increased in the two straight waveguides leading to a significant change in the amplitude of the transmittance curve (see Figure 5.16) with the change of RI of the sample. The change is near to linear which demonstrates the sensor's capability for the detection process and devices stability.

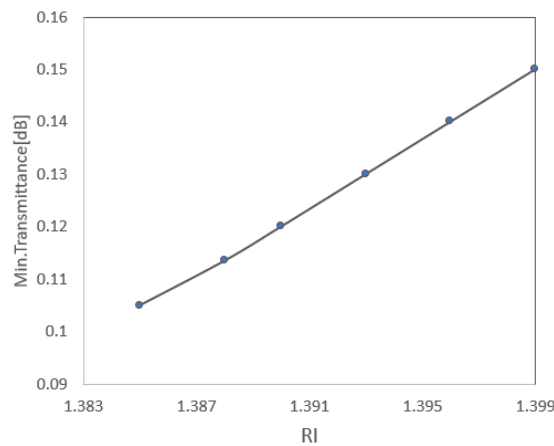


Fig.5.16: Change in amplitude of the transmittance curve due to change in RI.

The sensitivity of the sensor is significantly enhanced by the incorporation of two straight waveguides positioned on both sides coupled with a ring waveguide. This configuration leads to greater interaction between the light and the analyte(plasma). For light-analyte good interaction improves the system's ability to detect variations in refractive index (RI). However, the quality factor is 42 is lower than 62.11 [34]. As a result, the proposed sensor has a low quality factor but it offers high sensitivity that can significantly increase sensor detection capability.

## 5.2 Comparison Between WGM Ring Resonator, Silicon Photonics Ring Resonator, Nanocavity-Coupled Photonic Crystal Waveguide, and multi-core whispering gallery mode bio-sensor

Table 5.2.1: Sensitivity and Quality Factor of the Designed WGM Ring Resonator for Detecting Different Cancer Cells.

Cell name	Cell type	Refractive index (RI)	Sensitivity(S) (nm/RIU)	Quality Factor(Q)
Blood	Normal Cell	1.376	500	45
	Jurkat Cell	1.390		
Skin	Normal Cell	1.36	400	47.2
	Basal Cell	1.38		
Cervical	Normal Cell	1.368	1571	31.5
	Hela Cell	1.392		
Adrenal	Normal Cell	1.381	1175	33
	PC-12 Cell	1.395		
Breast	Normal Cell	1.385	500	42
	MDA-MB-231 Cell	1.399		

Table 5.2.2: Sensitivity and Quality Factor of the Designed Silicon Photonics Ring Resonator for Detecting Different Cancer Cells.

Cell name	Cell type	Refractive index (RI)	Sensitivity(S) (nm/RIU)	Quality Factor(Q)
Blood	Normal Cell	1.376	225.34	62.48
	Jurkat Cell	1.390		
Skin	Normal Cell	1.36	223.41	59.97
	Basal Cell	1.38		
Cervical	Normal Cell	1.368	225.51	62.27
	Hela Cell	1.392		
Adrenal	Normal Cell	1.381	226.22	62.06
	PC-12 Cell	1.395		
Breast	Normal Cell	1.385	227.54	62.11
	MDA-MB-231 Cell	1.399		

Table 5.2.3: Sensitivity and Quality Factor of the Designed Nanocavity-Coupled Photonic Crystal Waveguide for Detecting Different Cancer Cells.

Cell name	Cell type	Refractive index (RI)	Sensitivity(S) (nm/RIU)	Quality Factor(Q)
Blood	Normal Cell	1.376	390.5	4650
	Jurkat Cell	1.390		
Skin	Normal Cell	1.36	388.8	4870
	Basal Cell	1.38		

Cervical	Normal Cell	1.368	390.75	4500
	Hela Cell	1.392		
Adrenal	Normal Cell	1.381	390.95	4485
	PC-12 Cell	1.395		
Breast	Normal Cell	1.385	391.45	4445
	MDA-MB-231 Cell	1.399		

Table 5.2.4: Sensitivity and Quality Factor of the Designed multi-core whispering gallery mode bio-sensor for Detecting Different Cancer Cells.

Cell name	Cell type	Refractive index (RI)	Sensitivity(S) (nm/RIU)	Quality Factor(Q)
Blood	Normal Cell	1.376	--	--
	Jurkat Cell	1.390		
Skin	Normal Cell	1.36	650	--
	Basal Cell	1.38		
Cervical	Normal Cell	1.368	666.6667	--
	Hela Cell	1.392		
Adrenal	Normal Cell	1.381	--	--
	PC-12 Cell	1.395		
Breast	Normal Cell	1.385	642.857	--
	MDA-MB-231 Cell	1.399		



### 5.3 Discussion

The development of a highly optimized Whispering Gallery Mode (WGM) Ring Resonator (RR)-based biosensor presents a significant advancement in cancer detection technology. By incorporating a specially designed target plasma molecules recipient layer within the straight waveguide, the resonant light interacts with plasma molecules, inducing changes in the effective refractive index (RI). This enables precise detection and quantification of cancerous cells. The proposed biosensor undergoes rigorous numerical analysis using the finite element method within COMSOL Multiphysics to evaluate its spectral response and optimize its optical and structural parameters for enhanced performance.

The results indicate that the biosensor achieves high sensitivity across various cancer types according to the variations in the refractive index (RI) of plasma. The sensitivity (S) for Skin cancer cells (Basal) achieved 400 nm/RIU comparatively higher than other biosensors with a Quality factor (Q) of 47.2. While Cervical cancer cells (Hela) exhibit higher sensitivity (S) of 1571 nm/RIU with a Quality factor (Q) of 31.5. The Blood cancer cells (Jurkat) obtained a Sensitivity (S) of 500 nm/RIU with a Quality factor (Q) of 45. Finally, the adrenal gland cancer cells (PC-12) and breast cancer (MDA-MB-232) achieved sensitivities of 400 nm/RIU and 500 nm/RIU with quality factors (Q) 33 and 42, respectively.

The simulation and analysis demonstrate a higher sensitivity (S) compared to other biosensor-based designs but the Quality factor (Q) is slightly lower. As the Sensitivity is achieved higher, it significantly enhances the sensor's efficiency and reliability. The superior performance of this biosensor compared to existing biosensor-based designs highlights its potential for high-precision cancer diagnostics. The proposed WGM Ring Resonator biosensor demonstrates the significant advancements achieved for medical applications.

## **CHAPTER 6**

### **Conclusion and Future Work**

#### **6.1 Conclusion**

The proposed WGM biosensor in this study which is based on the ring-resonator presents a significant potential for the early detection of cancer by utilizing variations in the RI of plasma. This proposed sensor has achieved a remarkable sensitivity(S) and a quality factor(Q), as indicated by numerical analysis using the finite element method in COMSOL Multiphysics. The coupling efficiency between the light and analyte(plasma) using two straight waveguides leads to improved sensitivity than a single straight waveguide. Again, achieved higher sensitivity compared to Silicon Photonics Ring Resonators, Nanocavity-Coupled Photonic Crystal Waveguide, and multi-core whispering gallery mode bio-sensors highlighting the sensor efficiency and reliability. This proposed sensor offers a highly sensitive, cost-effective, non-invasive solution for advanced cancer detection technologies.

#### **6.2 Future Work**

- To design and simulate a 3D WGM Ring Resonator.
- To implement this simulation-based (WGM RR) device in real-life applications in diverse fields such as environmental monitoring, healthcare diagnostics, and industrial sensing.

## References

- [1] A. N. Oraevsky, “Whispering-gallery waves,” *Quantum Electron.*, vol. 32, no. 5, pp.377–400, 2002.
- [2] St. Paul’s Cathedral. Available: <https://www.stpauls.co.uk/>. [Accessed: Sept.07,2024].
- [3] M. A. Cooper, “Biosensor profiling of molecular interactions in pharmacology,” *Curr. Opin. Pharmacol.*, vol. 3, no. 5, pp. 557–562, 2003. doi: 10.1016/j.coph.2003.05.003.
- [4] T. Reynolds, “A Whispering Gallery Mode Microlaser Biosensor,” no. February, 2017.
- [5] D. M. El-Sherif, M. Abouzid, M. S. Gaballah, A. A. Ahmed, M. Adeel, and S. M. Sheta, “New approach in SARS-CoV-2 surveillance using biosensor technology: a review,” *Environ. Sci. Pollut. Res.*, vol. 29, no. 2, pp. 1677–1695, 2022. doi: 10.1007/s11356-021-17096-z.
- [6] A. Capocceffalo, S. Gentilini, L. Barolo, P. Baiocco, C. Conti, and N. Ghofraniha, “Biosensing with free space whispering gallery mode microlasers,” *Photonics Res.*, vol. 11, no. 5, pp. 732–741, 2023.
- [7] P. Steglich, M. Hülsemann, B. Dietzel, and A. Mai, “Optical biosensors based on silicon-on-insulator ring resonators: A review,” *Molecules*, vol. 24, no. 3, 2019. doi: 10.3390/molecules24030519.
- [8] M. S. Luchansky and R. C. Bailey, “High-Q optical sensors for chemical and biological analysis,” pp. 793–821, 2013.
- [9] S. M. Wildgen and R. C. Dunn, “Whispering gallery mode resonators for rapid label-free biosensing in small volume droplets,” *Biosensors*, vol. 5, no. 1, pp. 118–130, 2015. doi: 10.3390/bios5010118
- [10] Y. Sun and X. Fan, “Optical ring resonators for biochemical and chemical sensing,” *Anal. Bioanal. Chem.*, vol. 399, no. 1, pp. 205–211, 2011. doi: 10.1007/s00216-010-4237-z.
- [11] L. Pasquardini et al., “Whispering gallery mode aptasensors for detection of blood proteins,” *J. Biophotonics*, vol. 6, no. 2, pp. 178–187, 2013. doi: 10.1002/jbio.201200013.
- [12] R. Ahmed, A. A. Rifat, A. K. Yetisen, M. S. Salem, S. H. Yun, and H. Butt, “Optical microring resonator based corrosion sensing,” 2012.
- [13] R. Guider et al., “Design and optimization of SiON ring resonator-based biosensors for aflatoxin M1 detection,” *Sensors*, vol. 15, no. 7, pp. 17300–17312, 2015. doi: 10.3390/s150717300.
- [14] *Optical Ring Resonators: A Platform for Biological Sensing Applications*. Available: [www.jmss.mui.ac.ir](http://www.jmss.mui.ac.ir). [Accessed: Nov.16,2024].
- [15] A. K. Ajad, M. J. Islam, M. R. Kaysir, and J. Atai, “Highly sensitive biosensor based on WGM ring resonator for hemoglobin detection in blood samples,” *Optik*, vol. 226, 2021. doi: 10.1016/j.ijleo.2020.166009.
- [16] J. E. Heebner, V. Wong, A. Schweinsberg, R. W. Boyd, and D. J. Jackson, “Optical transmission characteristics of fiber ring resonators,” *IEEE J. Quantum Electron.*, vol. 40, no. 6, pp. 726–730, 2004. doi: 10.1109/JQE.2004.828232.
- [17] Y. Mao, F. Ren, D. Zhou, and Y. Li, “Highly sensitive PCF-SPR RI sensor for cancer detection using gold/graphene/Ti3C2Tx-MXene hybrid layer,” *Plasmonics*, 2024. doi: 10.1007/s11468-024-02467-2.
- [18] B. Lee, “Review of the present status of optical fiber sensors,” *Opt. Fiber Technol.*, vol. 9, no. 2, pp. 57–79, 2003. doi: 10.1016/S1068-5200(02)00527-8.
- [19] W. R. Heineman and W. B. Jensen, “Leland C. Clark Jr. (1918–2005),” *Biosens. Bioelectron.*, vol. 21, no. 8, pp. 1403–1404, 2006. doi: 10.1016/j.bios.2005.12.005.
- [20] F. Ligler and C. Taitt, “Optical Biosensors,” in *Opt. Biosens*, pp. 19–21, 2008. doi: 10.1016/B978-0-444-53125-4.X5001-3.
- [21] L. Castillo-Henríquez et al., “Biosensors for the detection of bacterial and viral clinical pathogens,” *Sensors*, vol. 20, no. 23, pp. 1–26, 2020. doi: 10.3390/s20236926.

- [22] J. M. Gamba, "The role of transport phenomena in whispering gallery mode optical biosensor performance," PhD Thesis, 2012.
- [23] D. Axelrod, T. P. Burghardt, and N. L. Thompson, "Total internal reflection fluorescence," Available: [www.annualreviews.org](http://www.annualreviews.org). [Accessed: Jan. 25, 2025].
- [24] R. J. Chen et al., "Noncovalent functionalization of carbon nanotubes for highly specific electronic biosensors," *Proc. Nat. Acad. Sci.*, vol. 101, no. 23, pp. 8331–8336, 2004. doi: 10.1073/pnas.0837064100.
- [25] J. I. Hahm and C. M. Lieber, "Direct ultrasensitive electrical detection of DNA and DNA sequence variations using nanowire nanosensors," *Nano Lett.*, vol. 4, no. 1, pp. 51–54, 2004. doi: 10.1021/nl034853b.
- [26] S. Panich et al., "Label-free Pb(II) whispering gallery mode sensing using self-assembled glutathione-modified gold nanoparticles on an optical microcavity," *Anal. Chem.*, vol. 86, no. 13, pp. 6299–6306, 2014. doi: 10.1021/ac500845h.
- [27] J. Zhu et al., "On-chip single nanoparticle detection and sizing by mode splitting in an ultrahigh-Q microresonator," *Nat. Photonics*, vol. 4, no. 1, pp. 46–49, 2010. doi: 10.1038/nphoton.2009.237.
- [28] A. B. Matsko and V. S. Ilchenko, "Optical resonators with whispering-gallery modes - Part I: Basics," *IEEE J. Select. Topics Quantum Electron.*, vol. 12, no. 1, pp. 3–14, 2006. doi: 10.1109/JSTQE.2005.862952.
- [29] M. R. Foreman, J. D. Swaim, and F. Vollmer, "Whispering gallery mode sensors: erratum," *Adv. Opt. Photon.*, vol. 7, no. 3, pp. 632, 2015. doi: 10.1364/aop.7.000632.
- [30] Q. Ma, T. Rossmann, and Z. Guo, "Temperature sensitivity of silica micro-resonators," *J. Phys. D Appl. Phys.*, vol. 41, no. 24, 2008. doi: 10.1088/0022-3727/41/24/245111.
- [31] P. Schneeweiss et al., "Fiber ring resonator with a nanofiber section for chiral cavity quantum electrodynamics and multimode strong coupling," *Opt. Lett.*, vol. 42, no. 1, pp. 85, 2017. doi: 10.1364/ol.42.000085.
- [32] C. Y. Chao and L. J. Guo, "Design and optimization of microring resonators in biochemical sensing applications," *J. Lightwave Technol.*, vol. 24, no. 3, pp. 1395–1402, 2006. doi: 10.1109/JLT.2005.863333.
- [33] G. C. Righini et al., "Whispering gallery mode microresonators: Fundamentals and applications," *Riv. Nuovo Cimento*, vol. 34, no. 7, pp. 435–488, 2011. doi: 10.1393/ncr/i2011-10067-2.
- [34] L. Ali, M. U. Mohammed, M. Khan, A. H. bin Yousuf, and M. H. Chowdhury, "High-Quality Optical Ring Resonator-Based Biosensor for Cancer Detection," *IEEE Sensors Journal*, vol. 20, no. 4, pp. 1867–1875, 2020. doi: 10.1109/JSEN.2019.2950664.
- [35] K. Chakrabarti, M. S. Obaidat, S. Mostufa, and A. K. Paul, "Design and analysis of a multi-core whispering gallery mode bio-sensor for detecting cancer cells and diabetes tear cells," 4, pp. 2294–2307, 2021.
- [36] S. Jindal, S. Sobti, M. Kumar, S. Sharma, and M. K. Pal, "Nanocavity-Coupled Photonic Crystal Waveguide as Highly Sensitive Platform for Cancer Detection," *IEEE Sensors Journal*, vol. 16, no. 10, pp. 3705–3710, 2016. doi: 10.1109/JSEN.2016.2536105.

## **Appendix**

### **Appendix A**

(Attach your code/ mathematical proof etc. here)

### **Appendix B**

(Attach your code/ mathematical proof etc. here)

### **Submitted Article in Conferences**

<b>Sl. No.</b>	<b>Description</b>	<b>Page</b>
1	Design of a WGM Ring Resonator Assisted Cancer Cell Detection System.	06